RÉPUBLIQUE FRANÇAISE
Liberté
Égalité
Fraternité

On the false alarm probability of the Normalized Matched Filter for off-grid target detection

IEEE ICASSP 2022

Pierre Develter[1,2], Jonathan Bosse[1], Olivier Rabaste[1], Philippe Forster[3], Jean-Philippe Ovarlez[1,2]

[1]ONERA, MATS [2]CentraleSupélec, SONDRA [3]Univ. Paris-Saclay, ENS Paris-Saclay, SATIE

April 5, 2022

Context: The Radar detection problem

- Primary goal of Radar systems: detect targets.
- Emit signal, and search for echoes in received signal.

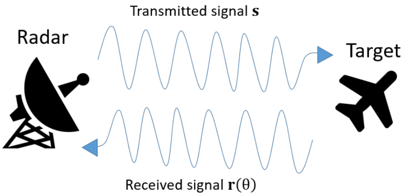

Context: The Radar detection problem

- Primary goal of Radar systems: detect targets.
- Emit signal, and search for echoes in received signal.

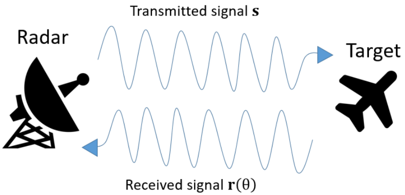

- Received signal depends on unknown target parameters θ.

Context: The Radar detection problem

- Primary goal of Radar systems: detect targets.
- Emit signal, and search for echoes in received signal.

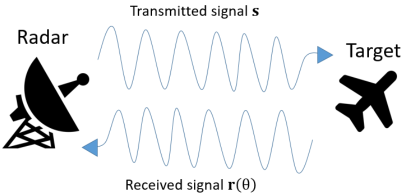

- Received signal depends on unknown target parameters θ.

Formalization: The Radar detection problem

The classical Radar detection problem is the following binary Hypothesis Test:

$$\begin{cases} H_0 : \mathbf{r} = \mathbf{n} \\ H_1 : \mathbf{r} = \alpha\, \mathbf{s}(\theta) + \mathbf{n} \end{cases}, \text{ where}$$

- $\mathbf{r} \in \mathbb{C}^N$ is the observation,
- $\mathbf{s}(\theta) \in \mathbb{C}^N$ is the signal echo reflected by a target with parameters θ (range, angle, Doppler...),
- $\alpha \in \mathbb{C}$ is the complex amplitude of the received signal,
- $\mathbf{n} \in \mathbb{C}^N$ is the additive noise vector, independent of the source signal. Our results hold for any spherically invariant distribution such as $\mathbf{n} \sim \mathcal{CN}(\mathbf{0}, \sigma^2\, \boldsymbol{\Gamma})$.

Formalization: The Radar detection problem

The classical Radar detection problem is the following binary Hypothesis Test:

$$\begin{cases} H_0 : \mathbf{r} = \mathbf{n} \\ H_1 : \mathbf{r} = \alpha\, \mathbf{s}(\theta) + \mathbf{n} \end{cases}, \text{ where}$$

- $\mathbf{r} \in \mathbb{C}^N$ is the observation,
- $\mathbf{s}(\theta) \in \mathbb{C}^N$ is the signal echo reflected by a target with parameters θ (range, angle, Doppler...),
- $\alpha \in \mathbb{C}$ is the complex amplitude of the received signal,
- $\mathbf{n} \in \mathbb{C}^N$ is the additive noise vector, independent of the source signal. Our results hold for any spherically invariant distribution such as $\mathbf{n} \sim \mathcal{CN}(\mathbf{0}, \sigma^2\, \boldsymbol{\Gamma})$.

$\mathbf{s}(\theta)$: General spectral analysis model (angle or Doppler with Radar) :

$$\mathbf{s}(\theta) = \frac{1}{\sqrt{N}} \left[1, e^{2i\pi\theta}, \ldots, e^{2i\pi(N-1)\theta}\right]^T.$$

The Generalized Likelihood Ratio Test

The Generalized Likelihood Ratio Test is given by:

$$\Lambda(\mathbf{r}) = \frac{\max\limits_{\boldsymbol{\lambda}_1} f_{H_1}(\mathbf{r})}{\max\limits_{\boldsymbol{\lambda}_0} f_{H_0}(\mathbf{r})} \underset{H_0}{\overset{H_1}{\gtrless}} \eta.$$

where

- for $i \in \{0, 1\}$, f_{H_i} is the density function of $\mathbf{r}$ under H_i and λ_i are the unknown parameters under H_i,
- η guarantees a fixed Probability of False Alarm (PFA).

The Normalized Matched Filter

- When $\lambda_1 = \{\sigma, \alpha\}$ and $\lambda_0 = \{\sigma\}$, with θ known, the GLRT reduces to the following Normalized Matched Filter (NMF) [Scharf and Lytle, 1971]:

$$t_{\boldsymbol{\Gamma}}(\mathbf{r}, \theta) = \frac{\left|\mathbf{s}(\theta)^H \boldsymbol{\Gamma}^{-1} \mathbf{r}\right|^2}{\left(\mathbf{s}(\theta)^H \boldsymbol{\Gamma}^{-1} \mathbf{s}(\theta)\right) \left(\mathbf{r}^H \boldsymbol{\Gamma}^{-1} \mathbf{r}\right)} \underset{H_0}{\overset{H_1}{\gtrless}} \eta.$$

The Normalized Matched Filter

- When $\lambda_1 = \{\sigma, \alpha\}$ and $\lambda_0 = \{\sigma\}$, with θ known, the GLRT reduces to the following Normalized Matched Filter (NMF) [Scharf and Lytle, 1971]:

$$t_{\Gamma}(\mathbf{r}, \theta) = \frac{\left|\mathbf{s}(\theta)^H \mathbf{\Gamma}^{-1} \mathbf{r}\right|^2}{\left(\mathbf{s}(\theta)^H \mathbf{\Gamma}^{-1} \mathbf{s}(\theta)\right) \left(\mathbf{r}^H \mathbf{\Gamma}^{-1} \mathbf{r}\right)} \underset{H_0}{\overset{H_1}{\gtrless}} \eta.$$

- Let us define the whitened and normalized versions of $\mathbf{s}(\theta)$ and $\mathbf{r}$:

$$\mathbf{s}(\theta) = \frac{\mathbf{\Gamma}^{-1/2} \mathbf{d}(\theta)}{\left(\mathbf{s}(\theta)^H \mathbf{\Gamma}^{-1} \mathbf{s}(\theta)\right)}$$

$$\mathbf{u} = \frac{\mathbf{\Gamma}^{-1/2} \mathbf{r}}{\left(\mathbf{r}^H \mathbf{\Gamma}^{-1} \mathbf{r}\right)}$$

- So that we can rewrite the NMF as:

$$t_{\Gamma}(\mathbf{r}, \theta) = \left|\mathbf{s}^H \mathbf{u}\right|^2 \underset{H_0}{\overset{H_1}{\gtrless}} \eta. \quad (1)$$

with $\mathbf{u}$ and $\mathbf{s}(\theta)$ on the unit complex N-sphere.

Mismatch and off-grid targets

- The NMF test quantity is the cosinus of the angle between $\mathbf{s}$ and $\mathbf{u}$.
- In practice, θ is unknown. Mismatch $\delta = \theta - \theta_0$ with θ_0 the test parameter.
- Whatever the signal power α value, if the mismatch is too big the signal is not detected.

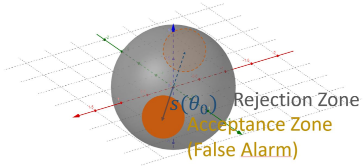

The Grid Principle

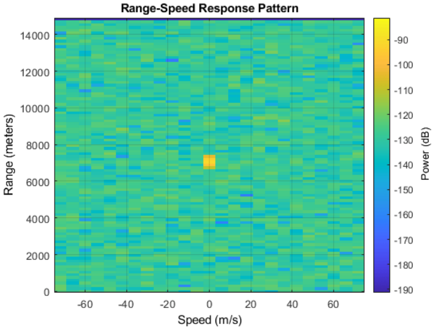

- The tests are run considering fixed values of θ in a grid G.
- In practice $\theta \neq \theta_0 \rightarrow$ mismatch $\rightarrow$ drop in detection performance.
- Grid cells : $\left[\frac{k}{N} - \frac{1}{2N}, \frac{k}{N} + \frac{1}{2N}\right]$, parameters $\theta_0 = \frac{k}{N}$

Impact of off-grid targets on the NMF

- The angle mismatch degrades the NMF response.
- θ uniformly distributed in a cell $\rightarrow$ Expected Probability of Detection (P_D): $\frac{\text{domain under threshold}}{\text{whole domain}}$

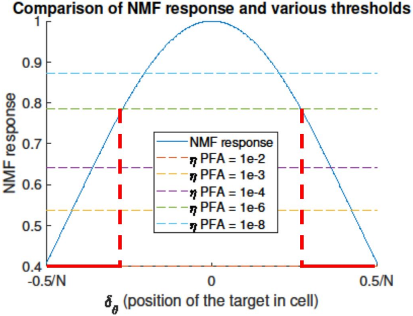

Impact of off-grid targets on the NMF

- The angle mismatch degrades the NMF response.
- θ uniformly distributed in a cell $\rightarrow$ Expected Probability of Detection (P_D): $\frac{\text{domain under threshold}}{\text{whole domain}}$
- $P_D \nrightarrow 1$ [Rabaste et al., 2016]
- It is even worse when $\Gamma \neq \mathbf{I}$

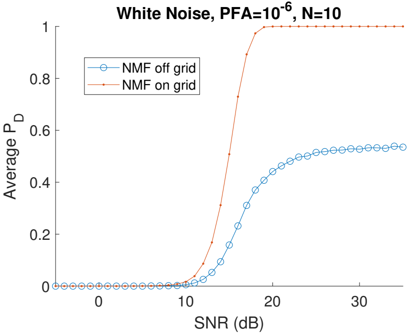

Existing Solutions

- Extension of the GLRT to off-grid targets:

$$\mathrm{GLRT}(\mathbf{r}, \theta_0) = \max_{\theta_c \in [\theta_0 - \Delta/2, \theta_0 + \Delta/2]} t_{\boldsymbol{\Gamma}}(\mathbf{r}, \theta_c) \underset{H_0}{\overset{H_1}{\gtrless}} \eta.$$

The best P_D, no closed form available, threshold unknown, precise approximation can be costly.

Existing Solutions

- Extension of the GLRT to off-grid targets:

$$\mathrm{GLRT}(\mathbf{r}, \theta_0) = \max_{\theta_c \in [\theta_0 - \Delta/2, \theta_0 + \Delta/2]} t_{\Gamma}(\mathbf{r}, \theta_c) \underset{H_0}{\overset{H_1}{\gtrless}} \eta.$$

  The best P_D, no closed form available, threshold unknown, precise approximation can be costly.

- Existing sub-optimal cost-efficient solutions include
  - Oversampling approximate GLRT, threshold unknown
  - Using DPSS subspace to approximate the cell structure, analytical threshold [Bosse and Rabaste, 2018]
  - Using a monopulse-inspired detection scheme that approximates the GLRT, no analytical threshold [Develter et al., 2021].

Existing Solutions

- Extension of the GLRT to off-grid targets:

$$\mathrm{GLRT}(\mathbf{r}, \theta_0) = \max_{\theta_c \in [\theta_0 - \Delta/2, \theta_0 + \Delta/2]} t_\Gamma(\mathbf{r}, \theta_c) \underset{H_0}{\overset{H_1}{\gtrless}} \eta.$$

  The best P_D, no closed form available, threshold unknown, precise approximation can be costly.

- Existing sub-optimal cost-efficient solutions include
  - Oversampling approximate GLRT, threshold unknown
  - Using DPSS subspace to approximate the cell structure, analytical threshold [Bosse and Rabaste, 2018]
  - Using a monopulse-inspired detection scheme that approximates the GLRT, no analytical threshold [Develter et al., 2021].
- These solutions do not correct the convergence issue for all Γ and are not always near GLRT. This motivates studies on the true GLRT.

Finding the P_{FA} of the NMF geometrically

- Since $\mathbf{u}$ is whitened, it is distributed uniformly over the whole sphere.
- Thus $P_{FA} = \frac{\text{Acceptance Zone Surface}}{\text{Rejection Zone Surface}}$.
- This gives: $P_{FA} = (1 - w^2)^{N-1}$.

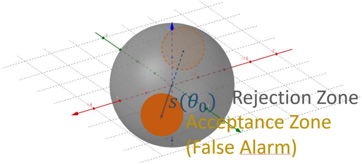

The NMF-GLRT

- The GLRT corresponding to the NMF when θ is considered as an unknown parameter over a search domain $\mathcal{D}$ gives:

$$\mathrm{GLRT}(\mathbf{r}, \mathcal{D}) = \max_{\theta_c \in \mathcal{D}} \left| \mathbf{s}(\theta_c)^H \mathbf{u} \right| \underset{H_0}{\overset{H_1}{\gtrless}} w'$$

The NMF-GLRT

- The GLRT corresponding to the NMF when θ is considered as an unknown parameter over a search domain $\mathcal{D}$ gives:

$$\mathrm{GLRT}(\mathbf{r}, \mathcal{D}) = \max_{\theta_c \in \mathcal{D}} \left| \mathbf{s}(\theta_c)^H \mathbf{u} \right| \underset{H_0}{\overset{H_1}{\gtrless}} w'$$

- The threshold is unknown, different from the NMF.
- It depends on the distribution of a continuum of non-independant variables $\rightarrow$ a priori hard to compute analytically.
- We use a geometrical method akin to the previous one.

Methodology for real signals

- Consider for now $\mathbf{u}$ and $\mathbf{s} \in \mathbb{R}^N$.
- $\mathbf{u}$ falls in the spherical cap $\mathcal{SC}_\theta$ corresponding to any $\theta \in \mathcal{D} \iff \mathbf{u} \in \bigcup_{\theta \in \mathcal{D}} \mathcal{SC}_\theta \rightarrow$ A target is detected

Methodology for real signals

- Consider for now $\mathbf{u}$ and $\mathbf{s} \in \mathbb{R}^N$.
- $\mathbf{u}$ falls in the spherical cap $\mathcal{SC}_\theta$ corresponding to any $\theta \in \mathcal{D} \iff \mathbf{u} \in \bigcup_{\theta \in \mathcal{D}} \mathcal{SC}_\theta \to$ A target is detected
- $\bigcup_{\theta \in \mathcal{D}} \mathcal{SC}_\theta$ forms a tube.

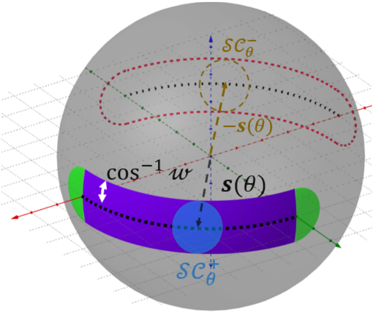

Methodology for real signals

- Consider for now $\mathbf{u}$ and $\mathbf{s} \in \mathbb{R}^N$.
- $\mathbf{u}$ falls in the spherical cap $\mathcal{SC}_\theta$ corresponding to any $\theta \in \mathcal{D} \iff \mathbf{u} \in \bigcup_{\theta \in \mathcal{D}} \mathcal{SC}_\theta \rightarrow$ A target is detected
- $\bigcup_{\theta \in \mathcal{D}} \mathcal{SC}_\theta$ forms a tube.
- Thanks to [Hotelling, 1939] we can compute the volume of this tube as the product of the cross section by the length of the curve.
- Valid as long as there is no overlap (the tube draws back into itself).

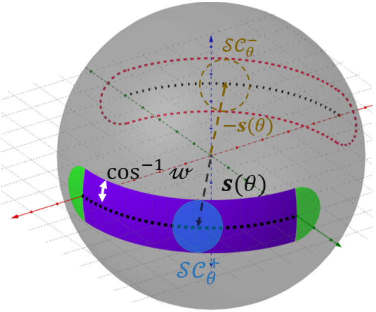

Rewriting our problem with real vectors

- Now $\mathbf{u}$ and $\mathbf{s} \in \mathbb{C}^{\mathrm{N}}$.
- $\left|\mathbf{s}(\theta)^{\mathrm{H}}\mathbf{u}\right| = \max_{\alpha} \mathrm{Re}\left(\mathbf{s}(\theta)^{\mathrm{H}}\mathbf{u}e^{-i\alpha}\right)$.
- Translating our problem to real signals $\rightarrow$ we have to maximize on the phase α of the product $\mathbf{s}(\theta)^{\mathrm{H}}\mathbf{u}$.

Rewriting our problem with real vectors

- Now $\mathbf{u}$ and $\mathbf{s} \in \mathbb{C}^N$.
- $\left|\mathbf{s}(\theta)^H \mathbf{u}\right| = \max_\alpha \operatorname{Re}\left(\mathbf{s}(\theta)^H \mathbf{u} e^{-i\alpha}\right)$.
- Translating our problem to real signals $\rightarrow$ we have to maximize on the phase α of the product $\mathbf{s}(\theta)^H \mathbf{u}$.
- In the end, we find that

$$\max_{\theta_c \in \mathcal{D}} \left|\mathbf{s}(\theta_c)^H \mathbf{u}\right| = \max_{\{\theta_c, \alpha\} \in \mathcal{D} \times [0, 2\pi]} \left(\boldsymbol{\gamma}_1(\theta_c) \cos\alpha + \boldsymbol{\gamma}_2(\theta_c) \sin\alpha\right)^T \underline{\mathbf{u}}$$

where $\boldsymbol{\gamma}_1(\theta_c) = \begin{bmatrix} \mathbf{s}_r(\theta_c) \\ \mathbf{s}_i(\theta_c) \end{bmatrix}$, $\boldsymbol{\gamma}_2(\theta_c) = \begin{bmatrix} -\mathbf{s}_i(\theta_c) \\ \mathbf{s}_r(\theta_c) \end{bmatrix}$ and $\underline{\mathbf{u}} = \begin{bmatrix} \mathbf{u}_r \\ \mathbf{u}_i \end{bmatrix}$ is a $2N$-real valued noise vector drawn uniformly on S^{2N-1} under H_0.

Methodology with complex signals

- We have to compute the volume of the tube around the 2D manifold $\boldsymbol{\gamma}(\alpha, \theta) = \boldsymbol{\gamma}_1(\theta)\,\cos\alpha + \boldsymbol{\gamma}_2(\theta)\,\sin\alpha$.

Methodology with complex signals

- We have to compute the volume of the tube around the 2D manifold $\boldsymbol{\gamma}(\alpha, \theta) = \boldsymbol{\gamma}_1(\theta) \cos\alpha + \boldsymbol{\gamma}_2(\theta) \sin\alpha$.
- Not covered by Hotelling, however [Johnstone and Siegmund, 1989] gives the following theorem:

Theorem

For $i \in [1, 2]$*, let* $\gamma_i : [0, t_0] \to S^{n-1}$ *be regular curves. Assume* $\boldsymbol{\gamma}_1(t)^T \boldsymbol{\gamma}_2(t) = 0$ *for all* t*. Let* $Z(t) = \left[\left(\boldsymbol{\gamma}_1(t)^T \mathbf{u}\right)^2 + \left(\boldsymbol{\gamma}_2(t)^T \mathbf{u}\right)^2\right]^{1/2}$ *where* $\mathbf{u}$ *is uniformly distributed on* S^{n-1}*. Then for* $0 < w < 1$*, we have:*

$$\mathbb{P}\left(\max_{0 \le t \le t_0} Z(t) > w\right) \le (1 - w^2)^{(n-2)/2} + \frac{\Gamma\left(\frac{n}{2}\right) w (1 - w^2)^{(n-3)/2}}{2\pi^{3/2}\,\Gamma\left(\frac{n-1}{2}\right)} \times \int_0^{t_0} \int_0^{2\pi} \left[\|\dot{\boldsymbol{\gamma}}_1(t) \cos\omega + \dot{\boldsymbol{\gamma}}_2(t) \sin\omega\|^2 - \left(\dot{\boldsymbol{\gamma}}_1(t)^T \boldsymbol{\gamma}_2(t)\right)^2\right]^{1/2} d\omega\, dt,$$

where $\dot{\boldsymbol{\gamma}}_i(t)$ *is the derivative of* $\boldsymbol{\gamma}_i(t)$ *with respect to* t*. When there is no overlap, this inequality becomes an equality.*

Final Results

Applying the previous theorem in our case, we get the following corollary :

Corollary

In the absence of overlap (low P_{FA} regimes), the P_{FA} for the NMF-GLRT for a search interval $\mathcal{D} = [\theta_1, \theta_2]$ with the steering vector $\mathrm{s}(\theta)$ defined previously is given by:

Final Results

Applying the previous theorem in our case, we get the following corollary :

Corollary

In the absence of overlap (low P_{FA} regimes), the P_{FA} for the NMF-GLRT for a search interval $\mathcal{D} = [\theta_1, \theta_2]$ with the steering vector $s(\theta)$ defined previously is given by:

- *Under white noise ($\boldsymbol{\Gamma} = \sigma^2 \mathbf{I}$):*

$$P_{FA} = \overbrace{(1 - w^2)^{N-1}}^{\text{on-grid relation}} + \sqrt{\frac{\pi}{3}} \frac{\Gamma(N)\, w\, (1 - w^2)^{N-\frac{3}{2}}}{\Gamma\left(N - \frac{1}{2}\right)} \left(N^2 - 1\right)^{\frac{1}{2}} \underbrace{(\theta_2 - \theta_1)}_{\text{length of search domain}} . \quad (2)$$

Final Results

Applying the previous theorem in our case, we get the following corollary :

Corollary

In the absence of overlap (low P_{FA} regimes), the P_{FA} for the NMF-GLRT for a search interval $\mathcal{D} = [\theta_1, \theta_2]$ with the steering vector $s(\theta)$ defined previously is given by:

- *Under white noise ($\boldsymbol{\Gamma} = \sigma^2 \mathbf{I}$):*

$$P_{FA} = \overbrace{(1 - w^2)^{N-1}}^{\text{on-grid relation}} + \sqrt{\frac{\pi}{3}} \frac{\Gamma(N)\, w\, (1 - w^2)^{N-\frac{3}{2}}}{\Gamma\left(N - \frac{1}{2}\right)} \left(N^2 - 1\right)^{\frac{1}{2}} \underbrace{(\theta_2 - \theta_1)}_{\text{length of search domain}} . \tag{2}$$

- *Under colored noise ($\boldsymbol{\Gamma} \neq \sigma^2 \mathbf{I}$), the integral in (2) can be evaluated numerically.*

Numerical evaluation

- Plot of the previous relation with $\boldsymbol{\Gamma} = \mathbf{I}$ against simulated threshold with 10^8 noise samples, $N = 10$, $\mathcal{D} = [0, 1/N]$, GLRT approximation with 30 tests.
- Low P_{FA} of practical interest in Radar $\rightarrow$ the formula fits perfectly.
- Very High P_{FA} $\rightarrow$ slight mismatch because of overlap phenomena.

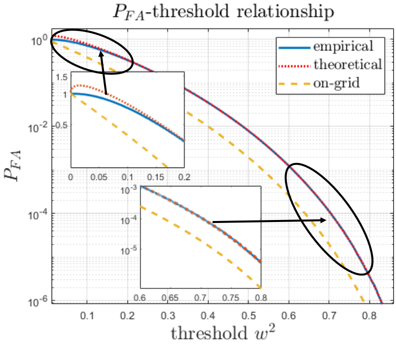

Conclusion

- In this work, we derived a P_{FA}-threshold relationship for the GLRT of the NMF extended to an unknown parameter of the target. It is exact for low P_{FA} of practical interest in Radar.
- Perspectives include the extension of this work to STAP (2D) detection and writing a journal paper deriving conditions under which no overlap arises.

References I

[Adler, 2000] Adler, R. J. (2000).
On excursion sets, tube formulas and maxima of random fields.
Annals of Applied Probability, pages 1–74.

[Bandiera et al., 2009] Bandiera, F., Orlando, D., and Ricci, G. (2009).
Advanced Radar Detection Schemes Under Mismatched Signal Models.
Morgan & Claypool publishers.

[Besson, 2006] Besson, O. (2006).
Detection of a signal in linear subspace with bounded mismatch.
Aerospace and Electronic Systems, IEEE Transactions on, 42(3):1131–1139.

[Bosse and Rabaste, 2018] Bosse, J. and Rabaste, O. (2018).
Subspace rejection for matching pursuit in the presence of unresolved targets.
Signal Processing, IEEE Transactions on, 66(8):1997–2010.

[Bosse et al., 2020] Bosse, J., Rabaste, O., and Ovarlez, J.-P. (2020).
Adaptive subspace detectors for off-grid mismatched targets.
ICASSP 2020-2020 IEEE International Conference on Acoustics, Speech and Signal Processing (ICASSP), pages 4777–4780.

[Chaumette, 2004] Chaumette, E. (2004).
Contribution à la caractérisation des performances des problèmes conjoints de détection et d'estimation.
PhD thesis, Cachan, Ecole Normale Superieure, Gif-sur-Yvette, France.

[Ciuonzo et al., 2016] Ciuonzo, D., De Maio, A., and Orlando, D. (2016).
A unifying framework for adaptive radar detection in homogeneous plus structured interference - part II: Detectors design.
Signal Processing, IEEE Transactions on, 64:2907–2919.

References II

[Conte et al., 1995] Conte, E., Lops, M., and Ricci, G. (1995).
Asymptotically optimum radar detection in compound-Gaussian clutter.
Aerospace and Electronic Systems, IEEE Transactions on, 31(2):617–625.

[De Maio et al., 2010] De Maio, A., Huang, Y., Palomar, D. P., Zhang, S., and Farina, A. (2010).
Fractional QCQP with applications in ML steering direction estimation for radar detection.
Signal Processing, IEEE Transactions on, 59(1):172–185.

[Develter et al., 2021] Develter, P., Bosse, J., Rabaste, O., Forster, P., and Ovarlez, J.-P. (2021).
Off-grid radar target detection with the normalized matched filter: A monopulse-based detection scheme.
In *2021 IEEE Statistical Signal Processing Workshop (SSP)*, pages 226–230. IEEE.

[Hohenwarter, 2002] Hohenwarter, M. (2002).
GeoGebra - ein Softwaresystem für dynamische Geometrie und Algebra der Ebene.
Diplomarbeit, Universität Salzburg.

[Hotelling, 1939] Hotelling, H. (1939).
Tubes and spheres in n-spaces, and a class of statistical problems.
American Journal of Mathematics, 61(2):440–460.

[Johnstone and Siegmund, 1989] Johnstone, I. and Siegmund, D. (1989).
On Hotelling's formula for the volume of tubes and Naiman's inequality.
The Annals of Statistics, pages 184–194.

[Knowles and Siegmund, 1989] Knowles, M. and Siegmund, D. (1989).
On Hotelling's approach to testing for a nonlinear parameter in regression.
International Statistical Review/Revue Internationale de Statistique, pages 205–220.

[Mosca, 1969] Mosca, E. (1969).
Angle estimation in amplitude comparison monopulse systems.
Aerospace and Electronic Systems, IEEE Transactions on, AES-5(2):205–212.

References III

[Ollila et al., 2012] Ollila, E., Tyler, D. E., Koivunen, V., and Poor, H. V. (2012).
Complex Elliptically Symmetric distributions: Survey, new results and applications.
Signal Processing, IEEE Transactions on, 60(11):5597 –5625.

[Pascal et al., 2006] Pascal, F., Ovarlez, J.-P., Forster, P., and Larzabal, P. (2006).
On a SIRV-CFAR detector with radar experimentations in impulsive noise.
In *European Signal Processing Conference, EUSIPCO'06*, Florence, Italy.

[Rabaste et al., 2016] Rabaste, O., Bosse, J., and Ovarlez, J.-P. (2016).
Off-grid target detection with Normalized Matched Subspace Filter.
In *24th European Signal Processing Conference (EUSIPCO)*, pages 1926–1930.

[Rabaste and Trouvé, 2014] Rabaste, O. and Trouvé, N. (2014).
Geometrical design of radar detectors in moderately impulsive noise.
Aerospace and Electronic Systems, IEEE Transactions on, 50(3):1938–1954.

[Scharf and Demeure, 1991] Scharf, L. L. and Demeure, C. (1991).
Statistical signal processing: detection, estimation, and time series analysis.
Prentice Hall.

[Scharf and Friedlander, 1994] Scharf, L. L. and Friedlander, B. (1994).
Matched subspace detectors.
Signal Processing, IEEE Transactions on, 42(8):2146–2157.

[Scharf and Lytle, 1971] Scharf, L. L. and Lytle, D. W. (1971).
Signal detection in Gaussian noise of unknown level: an invariance application.
Information Theory, IEEE Transactions on, 17:404–411.